




## RESEARCH LETTER

# The S-adenosylmethionine analog sinefungin inhibits the trimethylguanosine synthase TGS1 to promote telomerase activity and telomere lengthening

Alessandra Galati<sup>1</sup>, Livia Scatolini<sup>1</sup>, Emanuela Micheli<sup>1</sup>, Francesca Bavasso<sup>1</sup>, Alessandro Cicconi<sup>1</sup>, Paolo Maccallini<sup>1</sup>, Lu Chen<sup>2</sup> , Caitlin M. Roake<sup>3</sup>, Stefan Schoeftner<sup>4</sup>, Steven E. Artandi<sup>3</sup>, Maurizio Gatti<sup>1,5</sup>, Stefano Cacchione<sup>1</sup>  and Grazia D. Raffa<sup>1</sup> 

<sup>1</sup> Dipartimento di Biologia e Biotecnologie, Sapienza Università di Roma, Italy

<sup>2</sup> Cancer Signaling and Epigenetics Program-Cancer Epigenetics Institute, Fox Chase Cancer Center, Philadelphia, PA, USA

<sup>3</sup> Department of Medicine, Stanford University School of Medicine, Stanford, CA, USA

<sup>4</sup> Dipartimento di Scienze della Vita, Università degli studi di Trieste, Italy

<sup>5</sup> Istituto di Biologia e Patologia Molecolari del CNR, Roma, Italy

## Correspondence

S. Cacchione and G. D. Raffa, Dipartimento di Biologia e Biotecnologie, Sapienza Università di Roma, Roma, Italy  
 Tel: +39 06 49912238 (SC); +39 06 49912843 (GDR)  
 E-mails: stefano.cacchione@uniroma1.it; grazia.daniela.raffa@uniroma1.it

Alessandra Galati and Livia Scatolini contributed equally to this article.

(Received 16 October 2021, revised 16 October 2021, accepted 9 November 2021, available online 5 December 2021)

doi:10.1002/1873-3468.14240

Edited by Claus Azzalin

**Mutations in many genes that control the expression, the function, or the stability of telomerase cause telomere biology disorders (TBDs), such as dyskeratosis congenita, pulmonary fibrosis, and aplastic anemia. Mutations in a subset of the genes associated with TBDs cause reductions of the telomerase RNA moiety hTR, thus limiting telomerase activity. We have recently found that loss of the trimethylguanosine synthase TGS1 increases both hTR abundance and telomerase activity and leads to telomere elongation. Here, we show that treatment with the S-adenosylmethionine analog sinefungin inhibits TGS1 activity, increases the hTR levels, and promotes telomere lengthening in different cell types. Our results hold promise for restoring telomere length in stem and progenitor cells from TBD patients with reduced hTR levels.**

**Keywords:** hTR; RNA methyltransferase; RNA processing; Sinefungin; telomerase; telomerase reverse transcriptase (TERT); telomere; telomere biology disorders (TBDs); telomere lengthening; TGS1

Telomeres are specialized nucleoprotein structures at the extremities of linear chromosomes that serve at least two essential functions. They hide chromosome ends from being recognized as DNA breaks, preventing DNA damage response and fusion between free chromosome ends [1]. They also counterbalance loss of terminal sequences due to the inability of polymerases to replicate the linear DNA ends [2]. Human telomeres consist of repetitive short sequences that are bound

and protected by the shelterin complex [3] and maintained by the telomerase holoenzyme, whose core is formed by the TERT reverse transcriptase and the hTR RNA component that acts as template for the addition of TTAGGG repeats to the chromosome ends [4–7]. Telomerase activity is fine-tuned at several levels [4,6]. Telomerase is active in the germline and in stem and progenitor cells [8,9], but not in somatic cells, which undergo progressive telomere shortening [10,11].

## Abbreviations

AA, aplastic anemia; AdoMet, SAM, S-adenosylmethionine; DC, dyskeratosis congenita; GST, glutathione S-transferase; hTR, human telomerase RNA; PF, pulmonary fibrosis; TBD, telomere biology disorders; TGS1, trimethylguanosine synthase; TRAP assay, telomeric repeat amplification assay; TRF assay, telomere restriction fragment assay.

[Correction added on 10 May 2022, after first online publication: CRUI-CARE funding statement has been added.]

Maintaining proper telomere function and adequate length is essential to sustain proliferation of progenitor cells that ensure tissue renewal and homeostasis [12]. Germline mutations in several genes that control telomerase biogenesis and activity result in telomere biology disorders (TBDs), in which patients have telomeres shorter than age-matched healthy individuals. These diseases are caused by the exhaustion of progenitor cells in tissues such as skin, lungs, liver, and bone marrow [13–15]. They are heterogeneous in severity and can manifest at birth, in childhood, or at different adult ages. Remarkably, mutations leading to TBDs have been associated with every component of telomerase and with several regulators of telomerase activity [4,5,15–17].

Telomerase activity is mainly regulated by TERT expression that determines the cell types in which telomerase is present. Accordingly, many different *TERT* mutations have been identified that results in TBDs of different severity [15]. hTR is ubiquitously expressed but its level is also rate limiting for telomerase activity [18]. A subset of the TBDs, including dyskeratosis congenita (DC), aplastic anemia (AA), and pulmonary fibrosis (PF), are caused by mutations affecting hTR structure or biogenesis. Loss-of-function mutations in the *TERC* gene, which specifies hTR, dominantly reduce telomerase activity, resulting in TBDs [19–22]. Mutations in genes encoding the dyskerin components (*DKC1*, *NOP10*, *NHP2*, *NAF1*), a complex that binds and stabilizes hTR, also cause severe TBDs when homozygous [23]. In addition, TBDs are caused by mutations in genes that regulate hTR biogenesis such as *PARN* that specifies a deadenylase that removes post-transcriptionally added poly-A extensions from nascent *TERC* transcripts, protecting them from degradation by the exosome. Interestingly, the reduction in hTR level caused by *PARN* mutations is counteracted by mutations in *PAPD5* that encodes the poly-A polymerase that adenylates the hTR precursors. *PAPD5* KO cells show elevated hTR levels and increased telomerase activity compared with non-mutant cells, while *PAPD5* overexpression results in diminished hTR levels [24–29]. Consistent with this finding, RNAi-mediated *PAPD5* inhibition in *PARN*-depleted cells or in lines from patients carrying either *PARN* or *DKC1* mutations restore the hTR levels, telomerase activity, and telomere length [25,26,29,30]. These results were corroborated by recent work showing that chemical inhibition of *PAPD5* increases hTR levels and stimulates telomere lengthening in stem cells from DC patients [31] and human embryonic stem cells carrying DC-relevant mutations, thereby improving their hematopoietic differentiation potential [32].

Thus, drugs that increase the hTR levels are promising treatments for TBDs caused by reduced hTR amounts [31,32].

hTR biogenesis involves hypermethylation of its 5' monomethylguanosine cap to a tri-methylguanosine cap, a reaction catalyzed by the trimethylguanosine synthase 1 (TGS1) enzyme. We have recently shown that mutations in *TGS1* promote accumulation of mature hTR molecules both in the nucleus and in the cytoplasm, and increased telomerase activity and telomere lengthening in human cells [33]. Here, we show that treatment of different types of human cells with sinefungin, an S-adenosyl-methionine analog that inhibits TGS1 [34], mimics the effects of TGS1 depletion, increasing the hTR levels, telomerase activity, and telomere length compared to untreated cells. Thus, we identify a new compound that may be employed to ameliorate the self-renewal capacity of induced pluripotent stem cells (iPSCs) from TBD patients for autologous cell-based therapies.

## Materials and methods

### Methyltransferase assay

The *TGS1* coding sequence was cloned into the pGEX-6P vector and the construct used to transform *E. coli* BL21 strain (DE3). The bacterial strains expressing the GST fusion protein and GST alone were used to inoculate 1 liter of LB Broth containing ampicillin. IPTG at a concentration of 0.5 mM was added to induce protein expression when the culture was in exponential growth. After overnight incubation at RT with vigorous shaking, the bacterial cultures were centrifuged and the pellet lysed in 20 mL lysis buffer (Hepes 50 mM, pH 7.4, NaCl 0.2 M, EDTA 1 mM, NP40 0.5%, glycerol 5%) plus protease inhibitors and sonicated on ice. The lysate was centrifuged at 12 000 r.p.m. for 15 min at 4 °C, and the supernatant was incubated with glutathione-sepharose beads. Beads were washed 3 times with PBS/1% Triton X-100, 2 times with PBS, and finally resuspended in 1 mL GST-maintaining buffer (Tris 50 mM, pH 7.4, NaCl 0.1 M, EDTA 1 mM, glycerol 10%, DTT 1 mM) plus protease inhibitors. Protein concentrations were calculated using the Bradford assay (Sigma). The purity of the isolated proteins was verified by SDS/PAGE electrophoresis followed by Coomassie staining. Reaction was performed and data analyzed essentially as in ref. [35]. Reaction mixtures (20 µL) containing 50 mM Tris-HCl (pH 8.0), 5 mM DTT, 50 mM NaCl, 50 µM [<sup>3</sup>H-CH<sub>3</sub>]AdoMet (Perkin-Elmer NET155V), 5 mM m<sup>7</sup>GTP (Merck M6133), and 1 µg of GST-TGS1 were incubated for 2 h at 37 °C, in the presence or absence of 100 µM sinefungin (Merck S8559). A mock reaction was performed by incubating the mixture with GST-beads only. Aliquots (5 µL) were spotted

on polyethylene-imine cellulose TLC plates (Merck Z122882), in parallel with the reaction mixture alone containing [<sup>3</sup>H-CH<sub>3</sub>]AdoMet (No protein). The TLC plates were developed with 50 mM (NH<sub>4</sub>)<sub>2</sub>SO<sub>4</sub>. The lanes were cut into 13 1-cm strips, and the radioactivity was quantified by liquid scintillation counting.

## Cell cultures

UMUC3 cells [36] were cultured in EMEM EBSS supplemented with 2 mM glutamine, 0.1 mM nonessential amino acids, 10% fetal bovine serum, 1.5 g·L<sup>-1</sup> sodium bicarbonate, 1 mM sodium pyruvate as described in [33]; U2OS, BJ-HELT cells [37], *PARN* KO and control HeLa cells [29] were cultured in DMEM supplemented with 10% fetal bovine serum and penicillin–streptomycin at 37 °C, in 5% CO<sub>2</sub>. hBLAK Bladder Epithelium Progenitors (Cellntech) were cultured as recommended by manufacturer.

## Cell viability assay

Cumulative population doubling values were determined over a period of 30 days.  $1.5 \times 10^5$  cells·well<sup>-1</sup> were seeded in 6-well plates in duplicates and treated with 0–100 μM sinefungin. For calculation of doubling time, cells were harvested by trypsinization and counted by Burkert Haemocytometer Counting Chamber every 48/72 h.

## qRT-PCR

Total RNA was extracted with TRIzol reagent (Thermo Fisher Scientific, Waltham, MA, 15596026), treated with DNase I (RNase-free), and extracted with phenol/chloroform. The integrity of RNA samples was evaluated by gel electrophoresis. 1 μg of intact RNA (with a 28S:18S rRNA ratio = 2 : 1) was reverse transcribed with the RevertAid H Minus Reverse Transcriptase kit (Thermo Fisher Scientific, EP0451). Real-time PCRs were performed with Power up SYBR Green QPCR Master Mix (Thermo Fisher Scientific, A25742). The following primers were used: CGCTGTTT TTCTCGCTGACT (hTR Fw), GCTCTAGAATGAACG GTGGAA (hTR Rev), AGCCACATCGCTCAGACAC (GAPDH Fw), GCCCAATACGACCAAATCC (GAPDH Rev), AGCACCGTCTGCGTGAG (TERT Fw), CAGCT CGACGACGTACACAC (TERT Rev).

## Telomere Repeat Amplification Protocol (TRAP assay)

To measure telomerase activity, a two-step TRAP procedure was performed as in ref. [33]. Briefly, cell extracts were incubated with the telomeric primer (AATCCGTCGAG-CAGAGTT, TS primer) for a 30-min initial extension step at 30 °C in a PCR machine, followed by 5 min of

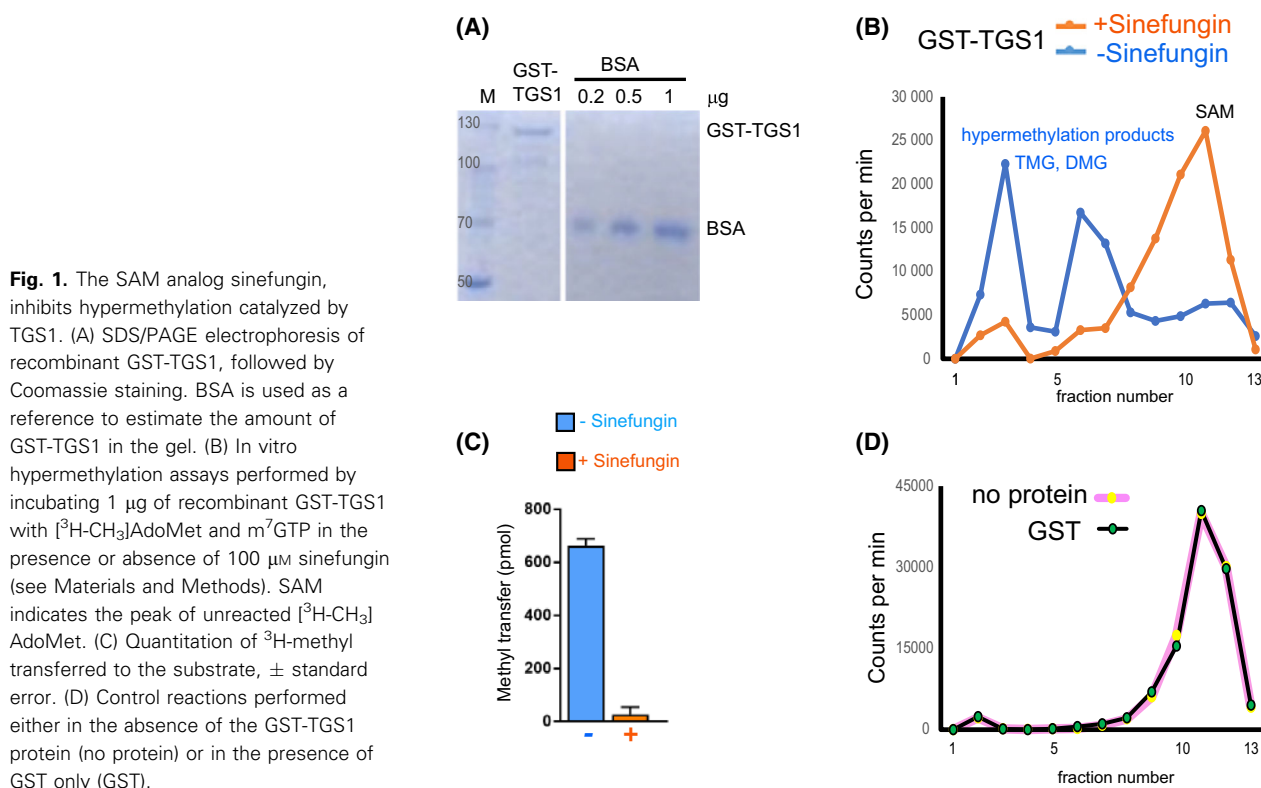
inactivation at 72 °C. 1 μL of the extended reaction was subjected to PCR amplification (24 cycle of 30 s at 94 °C, followed by 30 s at 59 °C) in the presence of primer mix (AATCCGTCGAGCAGAGTTAAAAGGCCGAGAAGC-GAT, TSNT; GCGCGGCTTACCCTTACCCTTACCCTAACC, ACX; ATCGCTTCTCGGCCTTTT, NT) and of <sup>32</sup>P end-labeled TS primer. The PCRs were resolved by 9% polyacrylamide gel electrophoresis at room temperature, and the gel was exposed to a phosphor-imager and scanned by a Typhoon scanner. Relative telomerase activity was quantified using ImageJ software, by pairwise comparison of the intensity of the first six amplicons in corresponding lanes with and without sinefungin, and averaging across the different dilutions for each sample.

## Telomere Restriction Fragment (TRF) Assay

Genomic DNA was digested overnight at 37 °C with HinfI and RsaI. For UMUC3 cells, 5 μg of digested DNA was loaded onto a 0.8% agarose gel (1× TBE) and separated by electrophoresis at 85 V for 16 h at room temperature. For *PARN* KO cells, 13 μg of digested DNA was loaded onto a 1.0% agarose gel (1× TBE) and separated by electrophoresis at 85 V for 12 h at room temperature. DNA was transferred to Hybond N membrane by upward capillary action and crosslinked to the membrane in an UV crosslinker. Standard Southern blotting procedure was carried out to detect telomeric restriction fragments using (CCCTAA)<sub>4</sub> oligonucleotide probe radioactively end-labeled. Calculation of telomere length was performed according to [38].

## Results

Prompted by our recent finding that mutations in *TGS1* increase the abundance of telomerase RNA and induce telomere elongation in living cells [33], we asked whether chemical inhibition of TGS1 activity could induce effects similar to those observed in *TGS1* mutant cells. It has been previously observed that the natural S-adenosyl methionine analog sinefungin suppresses TGS1 activity both *in vitro* and in living cells [34]. To further confirm that sinefungin inhibits the methyltransferase activity of TGS1, we performed an *in vitro* hypermethylation assay, as previously described [35,39]. Employing bacterially purified TGS1 fused to GST or GST alone, bound to glutathione beads (Fig. 1A), we performed *in vitro* methyltransferase assays in the presence or absence of sinefungin, using [<sup>3</sup>H-CH<sub>3</sub>]AdoMet as methyl donor and m<sup>7</sup>GTP as substrate. As shown in Fig. 1B, in reaction mixtures containing GST-TGS1 (blue line), we detected two peaks, most likely corresponding to the products of methyl transfer on the m<sup>7</sup>GTP substrate, which is



converted to m $^{2,7}$ GTP and m $^{2,2,7}$ GTP. In reactions containing no protein or GST beads only (Fig. 1D), a single peak was detected, most likely corresponding to the chromatographic mobility of [ $^3$ H-CH $_3$ ]AdoMet (SAM). Similarly, when 100  $\mu$ M sinefungin was added to the reaction mixtures, just a single peak comigrating with [ $^3$ H-CH $_3$ ]AdoMet was observed (Fig. 1B, orange line), indicating that sinefungin inhibits TGS1 methyl transfer activity (Fig. 1C).

We next asked whether TGS1 inhibition by sinefungin affects the abundance of hTR, which is upregulated in cells deficient for TGS1 [33]. hTR is constitutively expressed in human cells [40], yet hTR levels vary among different cell lines [41]. We first examined the effect of sinefungin treatment in UMUC3 bladder cancer cells.

In this cell line, telomeres are very short and the level of hTR is limiting for telomerase activity [36]. Indeed, the level of hTR in UMUC3 cells was significantly lower than that observed in HeLa cancer cells or in two immortalized cell lines (BJ-HELT and HEK293T; Fig. S1). It has been previously shown that an augment of the expression of hTR in UMUC3 cells increases telomerase activity and leads to a significant telomere lengthening [36]. We treated the UMUC3 line for 10 days with various concentrations of sinefungin (ranging from 12.5 to 100  $\mu$ M) and then assayed the levels of hTR RNA. hTR levels increased by 1.2 fold at lower concentrations of sinefungin (12.5–50  $\mu$ M) compared to mock-treated cells (Fig. 2A) and reached a 1.5-fold increase at 100  $\mu$ M.

**Fig. 2.** Sinefungin induces an increase in the hTR level and telomere lengthening in UMUC3 cells. (A) RT-qPCR measurements of hTR levels in UMUC3 cells treated with the indicated concentrations of sinefungin for 10 days. Bars represent fold change of hTR levels in treated vs untreated cells from three biological replicates, normalized to untreated cells and relative to GAPDH. Error bar, SEM; the *P* values were determined by one-way ANOVA. (B) Measurement of telomere length in UMUC3 cells by TRF analysis. TRF was carried out on genomic DNA extracted from cells treated or not with 100  $\mu$ M sinefungin for the indicated time in culture. Two independent experiments are reported. The numbers below the lanes indicate the average telomere length. Doubling times are shown in Fig. S2A. Note that sinefungin treatment induces substantial telomere lengthening. (C) Top, TRAP assay performed in 2X dilutions on extracts from UMUC3 cells treated or not with 50  $\mu$ M sinefungin for the indicated time. Bottom, quantification of TRAP activity. U2OS are telomerase-negative osteosarcoma cells used as negative control. Error bars, SD; a.u., arbitrary units; *P* values were determined by one-way ANOVA. (D) hTR levels determined by RT-qPCR on total RNA from control HeLa cells or a CRISPR-induced TGS1 mutant clone [33] (*TGS1 CRISPR M1*). Cells were treated or not with 100  $\mu$ M sinefungin. Bars represent fold change of hTR levels in treated vs untreated cells from three biological replicates, normalized to the control HeLa cell line and relative to GAPDH. Error bar, SEM; *P* values were determined by one-way ANOVA.

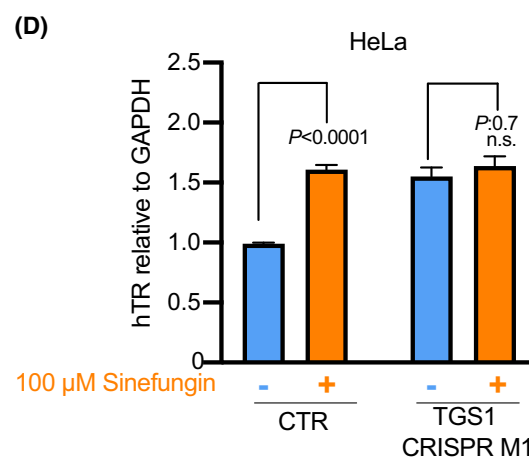
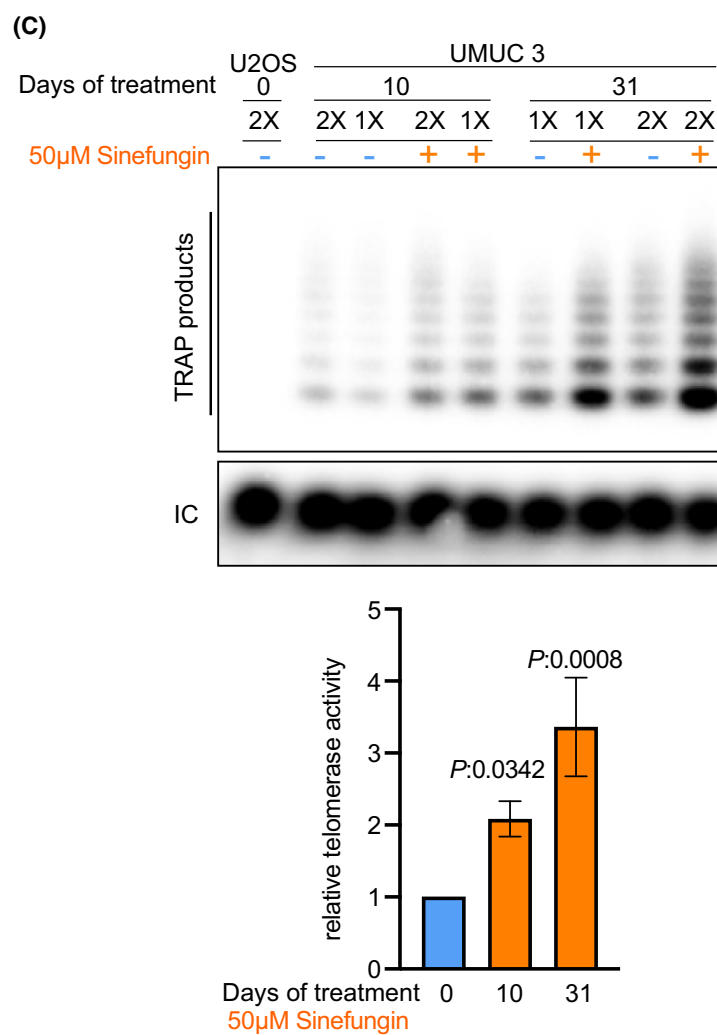
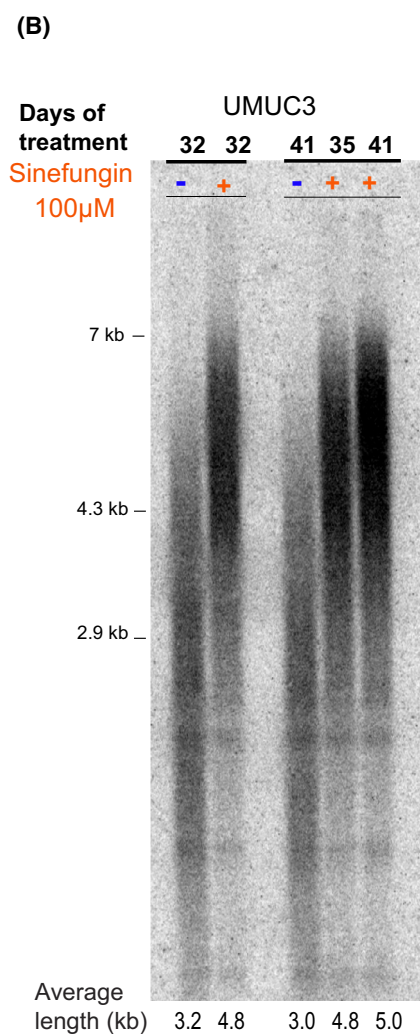
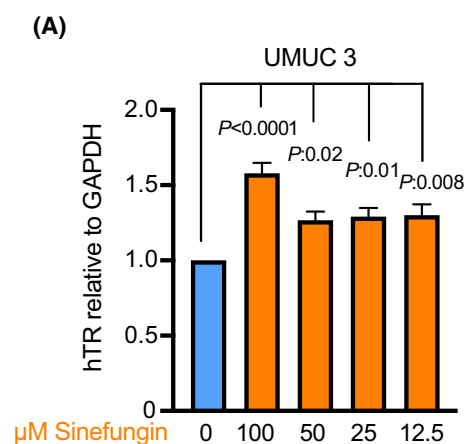






**Fig. 3.** Sinefungin increases the hTR level and telomere length in *PARN* KO cells. (A) Western blot showing that *PARN* KO mutant HeLa cells have a strongly reduced *PARN* level. (B) RT-qPCR measurements of hTR levels in control and in *PARN* KO mutant HeLa cells, treated with the indicated concentrations of sinefungin for 10 days. Bars represent fold change of hTR levels in treated vs untreated cells from three biological replicates, normalized to the control HeLa cell line and relative to GAPDH. Error bar, SEM; the *P* value was determined by one-way ANOVA. (C) Top, TRAP assay performed in 2× dilutions on extracts from control and *PARN* KO cells treated or not with 50 μM sinefungin for 13 days. Bottom, quantification of TRAP activity. Error bars, SD; a.u., arbitrary units; *P* values were determined by one-way ANOVA. (D) TRF analysis carried out on genomic DNA from cells treated or not with sinefungin (50 μM) for 46 days. The numbers below the lanes indicate the average telomere length. Untreated and treated cell lines showed similar doubling times.

Consistent with this result, telomere restriction fragment (TRF) analysis showed an increase in telomere length in UMUC3 cells grown in the presence of 100 μM sinefungin for over 30 days (over 15 population doublings; Fig. 2B and Fig. S2A). Population doubling analysis showed that different concentrations of sinefungin do not result in significant toxic effects on UMUC3 cells in the first 10 days of treatment. However, during the long-term treatments, the growth rate decreased with increasing drug concentrations (Fig. S2A). We then performed telomeric repeat amplification (TRAP) assay in UMUC3 cells treated for 10 and 31 days with 50 μM sinefungin and found that telomerase activity was increased by 2- and 3-fold, respectively, compared to untreated cells (Fig. 2C). This increase is due to an augmented hTR dosage, as the hTERT levels were not significantly changed after 10 days of treatment with 50 μM sinefungin (Fig. S2B). These results indicate that the effect of chemical inhibition of TGS1 on the hTR level is comparable to that elicited by *TGS1* mutations. Next, we compared the effects of sinefungin treatment in cells either proficient or deficient for TGS1. As previously reported [33], the *TGS1* CRISPR M1 HeLa cell line carries CRISPR-induced mutations in *TGS1* and has a 1.5-fold increase in hTR levels, compared to the control (CTR). Treatment with 100 μM sinefungin induced a 1.5-fold increase in hTR levels in control cells, but not in *TGS1* CRISPR M1 mutant cells (Fig. 2D; compare untreated cells with sinefungin-treated cells), indicating that modulation of the hTR levels by sinefungin requires functional TGS1.

We finally tested the effects of sinefungin on HeLa cells carrying mutations in the *PARN* deadenylase-coding gene (*PARN* KO), one of the factors responsible for dyskeratosis congenita, pulmonary fibrosis, and/or bone marrow failure [42–44]. The *PARN* KO HeLa cells are characterized by shortened telomeres, owing to reduced levels of telomerase RNA [29] (Fig. 3A and B). After a 10-day treatment with sinefungin, the hTR levels were significantly increased in the *PARN* KO cells treated with 25–100 μM sinefungin, compared to mock-treated cells (Fig. 3B). A dose-dependent

increase in hTR was evident also in control HeLa cells (Fig. 3B). We also evaluated the growth rates of CTRL and *PARN* KO cells in response to different doses of sinefungin (Fig. S3A,B). The cell viability of control or *PARN* KO cells was not strongly affected by sinefungin concentrations up to 50 μM, whereas 100 μM sinefungin induced a strong decrease in the growth rate of *PARN* KO cells (Fig. S3B) and a minor decrease in control cells (Fig. S3A).

In *PARN* KO cells, telomerase activity was reduced by 50%, compared to control cells (Fig. 3C and ref [29]). In response to treatment with 50 μM sinefungin for 13 days, telomerase activity was increased by 2.3 fold in *PARN* KO cells and by 1.6 fold in control cells (Fig. 3C), with no significant variation in hTERT levels (Fig. S3C). Furthermore, substantial telomere lengthening was observed after 46 days of treatment with 50 μM sinefungin of *PARN* KO cells (Fig. 3D). Overall, these results indicate that sinefungin-induced TGS1 inhibition results in higher hTR levels and increased telomerase activity.

## Discussion

Our results clearly show that sinefungin inhibits the methyltransferase activity of TGS1, increases the hTR level, and promotes telomere elongation in both UMUC3 and HeLa cells, characterized by short and long telomeres, respectively. In addition, we demonstrated that sinefungin elongates the telomeres of cells bearing mutations in the *PARN* gene, which promotes hTR biogenesis and is responsible for DC and pulmonary fibrosis [42–44]. The increase in hTR observed in cells treated with sinefungin is caused by reduced activity of TGS1. We have previously shown that TGS1 downregulates the levels of hTR, likely by restricting hTR localization to Cajal bodies and preventing its export to the cytoplasm and degradation by RNA surveillance activities [33]. Similar to what has been observed in cells deficient for TGS1, also in cells treated with sinefungin, the surplus of hTR that escaped degradation could be assembled into functional telomerase, leading to telomere elongation.

Very recent work has shown that chemical inhibition (with the BCH001 and RG7834 dihydroquinolizinones) of PAPD5 increases the hTR levels and promotes telomere elongation in different cell types deficient for either PARN or DKC1 [31,32]. Thus, both sinefungin and the chemical inhibitors of PAPD5, by acting on different protein targets, promote telomere elongation in cells with reduced levels of hTR.

Chemical inhibitors of PAPD5 were also administered to mice bearing transplanted human hematopoietic cells with mutations in the *PARN* gene. Mice treated for 6 weeks with RG7834 supplied in drinking water displayed significant increases in hTR and telomere length in transplanted human cells, compared with the human cells grown in untreated mice. These experiments also showed RG7834 administration does not affect human hematopoietic cell engraftment and does not cause adverse effects to mice [31]. Our results lead us to believe that it would be worth performing similar experiments with sinefungin to determine whether this drug can restore the telomere length and hematopoietic potential of stem cells without major toxic effects to mice, as it does PAPD5 inhibition [32].

Sinefungin is a general inhibitor of SAM-dependent methyltransferases that has both antimicrobial [45] and antiviral properties [46,47]. Sinefungin suppresses the MTase activity of the nsp16 2'-O-RNA methyltransferase from SARS-COV-2, a finding that prompted the development of drug discovery screens for compounds that could be used to contain viral infection [48–52]. In addition, sinefungin is a potent inhibitor of different parasitic protozoa [53–57], and a candidate therapeutic agent for treatment of CBS-deficient homocystinuria [58] and renal fibrosis [59]. These multiple therapeutic properties of sinefungin stimulated searches for its chemical analogs, so as to devise tailored treatments with optimized efficiency and tolerability [60–68]. Some of these compounds could now be tested on cells and animal models bearing mutations in TBD genes to identify the most suitable candidates for therapy of different short telomere diseases.

In summary, our finding that sinefungin inhibits TGS1 activity and promotes telomere elongation in human cells offers a new opportunity to upregulate telomere length in cells with pathologically short telomeres. Given the genetic heterogeneity of TBDs [16], it is also possible to envisage specific or combined uses of sinefungin and PAPD5 inhibitors for precision treatments of different short telomere conditions, depending on the underlying molecular defect leading to telomere shortening.

## Acknowledgements

Fondazione Telethon (Telethon Foundation): GDR GPP13147. Agenzia Spaziale Italiana (ASI): SC 2016-6-U0. Associazione Italiana per la Ricerca sul Cancro (AIRC): MG IG 20528. Associazione Italiana per la Ricerca sul Cancro (AIRC): SS IG18381 and IG 23074. European Union, European Regional Development Fund and Interreg V-A Italia-Austria 2014–2020: SS ITAT1096-P and ITAT1050. Open Access Funding provided by Università degli Studi di Roma La Sapienza within the CRUI-CARE Agreement.

## Conflict of interest

GDR, SC, and SS are named as inventors on patent applications relating to chemically inhibiting TGS1 in telomere diseases.

## Data accessibility

The data that support the finding of this study are available in the figures and the supplementary material of this article.

## Author contributions

AG, SEA, MG, SC, and GDR conceptualization; AGEM, LC, CMR, SC, and GDR data curation; SS, SEA, MG, SC, and GDR formal analysis; AG, EM, FB, AC, PM, LS, LC, CMR, SC, and GDR investigation; MG, SC, and GDR writing original draft; AG, EM, FB, AC, PM, LS, LC, CMR, SS, SEA, MG, SC, and GDR writing-review and editing; SS, MG, SC, and GDR funding acquisition; MG, SC, and GDR supervision.

## References

- 1 Lazzerini-Denchi E and Sfeir A. (2016) Stop pulling my strings — what telomeres taught us about the DNA damage response. *Nat Rev Mol Cell Biol* **17**, 364–378.
- 2 Shay JW and Wright WE (2019) Telomeres and telomerase: three decades of progress. *Nat Rev Genet* **20**, 299–309.
- 3 de Lange T (2018) Shelterin-mediated telomere protection. *Annu Rev Genet* **52**, 223–247.
- 4 Roake CM and Artandi SE (2020) Regulation of human telomerase in homeostasis and disease. *Nat Rev Mol Cell Biol* **21**, 384–397.
- 5 Smith EM, Pendlebury DF and Nandakumar J (2020) Structural biology of telomeres and telomerase. *Cell Mol Life Sci* **77**, 61–79.



- 6 Nguyen THD, Collins K and Nogales E (2019) Telomerase structures and regulation: shedding light on the chromosome end. *Curr Opin Struct Biol* **55**, 185–193.
- 7 Wu RA, Upton HE, Vogan JM and Collins K (2017) Telomerase mechanism of telomere synthesis. *Annu Rev Biochem* **86**, 439–460.
- 8 Wright WE, Piatyszek MA, Rainey WE, Byrd W and Shay JW (1996) Telomerase activity in human germline and embryonic tissues and cells. *Dev Genet* **18**, 173–179.
- 9 Yui J, Chiu CP and Lansdorp PM (1998) Telomerase activity in candidate stem cells from fetal liver and adult bone marrow. *Blood* **91**, 3255–3262.
- 10 Bodnar AG, Ouellette M, Frolkis M, Holt SE, Chiu C-P, Morin GB, Harley CB, Shay JW, Lichtsteiner S and Wright WE (1998) Extension of life-span by introduction of telomerase into normal human cells. *Science* **279**, 349–352.
- 11 Allsopp RC, Morin GB, DePinho R, Harley CB and Weissman IL (2003) Telomerase is required to slow telomere shortening and extend replicative lifespan of HSCs during serial transplantation. *Blood* **102**, 517–520.
- 12 Hao LY, Armanios M, Strong MA, Karim B, Feldser DM, Huso D and Greider CW (2005) Short telomeres, even in the presence of telomerase, limit tissue renewal capacity. *Cell* **123**, 1121–1131.
- 13 Niewisch MR and Savage SA (2019) An update on the biology and management of dyskeratosis congenita and related telomere biology disorders. *Exp Rev Hematol* **12**, 1037–1052.
- 14 Opreko PL and Shay JW (2017) Telomere-associated aging disorders. *Ageing Res Rev* **33**, 52–66.
- 15 Grill S and Nandakumar J (2020) Molecular mechanisms of telomere biology disorders. *J Biol Chem* **296**, 100064.
- 16 Bertuch AA (2016) The molecular genetics of the telomere biology disorders. *RNA Biol* **13**, 696–706.
- 17 Nagpal N and Agarwal S (2020) Telomerase RNA processing: Implications for human health and disease. *Stem Cells* **10**, 3270.
- 18 Greider CW (2006) Telomerase RNA levels limit the telomere length equilibrium. *Cold Spring Harb Symp Quant Biol* **71**, 225–229.
- 19 Aubert G, Baerlocher GM, Vulto I, Poon SS and Lansdorp PM (2012) Collapse of telomere homeostasis in hematopoietic cells caused by heterozygous mutations in telomerase genes. *PLoS Genet* **8**, e1002696.
- 20 Marrone A, Stevens D, Vulliamy T, Dokal I and Mason PJ (2004) Heterozygous telomerase RNA mutations found in dyskeratosis congenita and aplastic anemia reduce telomerase activity via haploinsufficiency. *Blood* **104**, 3936–3942.
- 21 Vulliamy T, Marrone A, Goldman F, Dearlove A, Bessler M, Mason PJ and Dokal I (2001) The RNA component of telomerase is mutated in autosomal dominant dyskeratosis congenita. *Nature* **413**, 432–435.
- 22 Wong JM and Collins K (2006) Telomerase RNA level limits telomere maintenance in X-linked dyskeratosis congenita. *Genes Dev* **20**, 2848–2858.
- 23 Dokal I, Vulliamy T, Mason P and Bessler M (2011) Clinical utility gene card for: dyskeratosis congenita. *Eur J Hum Genet* **19**, 3–4.
- 24 Tseng CK, Wang H-F, Burns AM, Schroeder MR, Gaspari M and Baumann P (2015) Human telomerase RNA processing and quality control. *Cell Rep* **13**, 2232–2243.
- 25 Boyraz B, Moon DH, Segal M, Muosieyiri MZ, Aykanat A, Tai AK, Cahan P and Agarwal S (2016) Posttranscriptional manipulation of TERC reverses molecular hallmarks of telomere disease. *J Clin Investig* **126**, 3377–3382.
- 26 Shukla S, Schmidt JC, Goldfarb KC, Cech TR and Parker R (2016) Inhibition of telomerase RNA decay rescues telomerase deficiency caused by dyskerin or PARN defects. *Nat Struct Mol Biol* **23**, 286–292.
- 27 Nguyen D, Grenier St-Sauveur V, Bergeron D, Dupuis-Sandoval F, Scott MS and Bachand F (2015) A polyadenylation-dependent 3' end maturation pathway is required for the synthesis of the human telomerase RNA. *Cell Rep* **13**, 2244–2257.
- 28 Son A, Park JE and Kim VN (2018) PARN and TOE1 constitute a 3' end maturation module for nuclear non-coding RNAs. *Cell Rep* **23**, 888–898.
- 29 Roake CM, Chen L, Chakravarthy AL, Ferrell JE, Raffa GD and Artandi SE (2019) Disruption of Telomerase RNA maturation kinetics precipitates disease. *Mol Cell* **74**, 688–700.
- 30 Fok WC, Shukla S, Vessoni AT, Brenner KA, Parker R, Sturgeon CM and Batista LFZ (2019) Posttranscriptional modulation of TERC by PAPD5 inhibition rescues hematopoietic development in dyskeratosis congenita. *Blood* **133**, 1308–1312.
- 31 Nagpal N, Wang J, Zeng J, Lo E, Moon DH, Luk K, Braun RO, Burroughs LM, Keel SB, Reilly C *et al.* (2020) Small-molecule PAPD5 inhibitors restore telomerase activity in patient stem cells. *Cell Stem Cell* **26**, 896–909.
- 32 Shukla S, Jeong HC, Sturgeon CM, Parker R and Batista LFZ (2020) Chemical inhibition of PAPD5/7 rescues telomerase function and hematopoiesis in dyskeratosis congenita. *Blood Adv* **4**, 2717–2722.
- 33 Chen L, Roake CM, Galati A, Bavasso F, Micheli E, Saggio I, Schoeftner S, Cacchione S, Gatti M, Artandi SE *et al.* (2020) Loss of human TGS1 hypermethylase promotes increased telomerase RNA and telomere elongation. *Cell Rep* **30**, 1358–1372.
- 34 Yedavalli VS and Jeang KT (2010) Trimethylguanosine capping selectively promotes expression of Rev-dependent HIV-1 RNAs. *Proc Natl Acad Sci USA* **107**, 14787–14792.

- 35 Hausmann S and Shuman S (2005) Specificity and mechanism of RNA cap guanine-N2 methyltransferase (Tgs1). *J Biol Chem* **280**, 4021–4024.
- 36 Xu L and Blackburn EH (2007) Human cancer cells harbor T-stumps, a distinct class of extremely short telomeres. *Mol Cell* **28**, 315–327.
- 37 Hahn WC, Stewart SA, Brooks MW, York SG, Eaton E, Kurachi A, Beijersbergen RL, Knoll JHM, Meyerson M and Weinberg RA (1999) Inhibition of telomerase limits the growth of human cancer cells. *Nat Med* **5**, 1164–1170.
- 38 Lincz LF, Scorgie FE, Garg MB, Gilbert J and Sakoff JA (2020) A simplified method to calculate telomere length from Southern blot images of terminal restriction fragment lengths. *Biotechniques* **68**, 28–34.
- 39 Hausmann S, Zheng S, Costanzo M, Brost RL, Garcin D, Boone C, Shuman S and Schwer B (2008) Genetic and biochemical analysis of yeast and human cap trimethylguanosine synthase: functional overlap of 2,2,7-trimethylguanosine caps, small nuclear ribonucleoprotein components, pre-mRNA splicing factors, and RNA decay pathways. *J Biol Chem* **283**, 31706–31718.
- 40 Avilion AA (1996) Human telomerase RNA and telomerase activity in immortal cell lines and tumor tissues. *Can Res* **56**, 645–650.
- 41 Yi X, Shay JW and Wright WE (2001) Quantitation of telomerase components and hTERT mRNA splicing patterns in immortal human cells. *Nucleic Acids Res* **29**, 4818–4825.
- 42 Stuart BD, Choi J, Zaidi S, Xing C, Holohan B, Chen R, Choi M, Dharwadkar P, Torres F, Girod CE *et al.* (2015) Exome sequencing links mutations in PARN and RTEL1 with familial pulmonary fibrosis and telomere shortening. *Nat Genet* **47**, 512–517.
- 43 Dhanraj S (2015) Bone marrow failure and developmental delay caused by mutations in poly(A)-specific ribonuclease (PARN). *J Med Genet* **52**, 738–748.
- 44 Tummala H, Walne A, Collopy L, Cardoso S, de la Fuente J, Lawson S, Powell J, Cooper N, Foster A, Mohammed S *et al.* (2015) Poly(A)-specific ribonuclease deficiency impacts telomere biology and causes dyskeratosis congenita. *J Clin Invest* **125**, 2151–2160.
- 45 Yadav MK, Park SW, Chae SW and Song JJ (2014) Sinefungin, a natural nucleoside analogue of S-adenosylmethionine, inhibits *Streptococcus pneumoniae* biofilm growth. *Biomed Res Int* **2014**, 156987.
- 46 Zhao Z, Martin C, Fan R, Bourne PE and Xie L (2016) Drug repurposing to target Ebola virus replication and virulence using structural systems pharmacology. *BMC Bioinformatics* **17**, 90.
- 47 Hercik K, Brynda J, Nencka R and Boura E (2017) Structural basis of Zika virus methyltransferase inhibition by sinefungin. *Arch Virol* **162**, 2091–2096.
- 48 Chen Y and Guo D (2016) Molecular mechanisms of coronavirus RNA capping and methylation. *Virol Sin* **31**, 3–11.
- 49 Decroly E, Debarnot C, Ferron F, Bouvet M, Coutard B, Imbert I, Gluais L, Papageorgiou N, Sharff A, Bricogne G *et al.* (2011) Crystal structure and functional analysis of the SARS-coronavirus RNA cap 2'-O-methyltransferase nsp10/nsp16 complex. *PLoS Pathog* **7**, e1002059.
- 50 Tazikeh-Lemeski E, Moradi S, Raoufi R, Shahlaei M, Janlou MAM and Zolghadri S (2020) Targeting SARS-COV-2 non-structural protein 16: a virtual drug repurposing study. *J Biomol Struct Dyn* **39**, 4633–4646.
- 51 Krafcikova P, Silhan J, Nencka R and Boura E (2020) Structural analysis of the SARS-CoV-2 methyltransferase complex involved in RNA cap creation bound to sinefungin. *Nat Commun* **11**, 3717.
- 52 Rosas-Lemus M (2020) High-resolution structures of the SARS-CoV-2 2'-O-methyltransferase reveal strategies for structure-based inhibitor design. *Sci Signal* **13**, 1202.
- 53 Bhattacharya A (2019) Genomewide analysis of mode of action of the S-adenosylmethionine analogue sinefungin in *Leishmania infantum*. *mSystems* **4**, 19.
- 54 McNally KP and Agabian N (1992) Trypanosoma brucei spliced-leader RNA methylations are required for trans splicing in vivo. *Mol Cell Biol* **12**, 4844–4851.
- 55 Trager W, Tershakovec M, Chiang PK and Cantoni GL (1980) Plasmodium falciparum: antimalarial activity in culture of sinefungin and other methylation inhibitors. *Exp Parasitol* **50**, 83–89.
- 56 Ferrante A, Ljungstrom I, Hultdt G and Lederer E (1984) Amoebicidal activity of the antifungal antibiotic sinefungin against *Entamoeba histolytica*. *Trans R Soc Trop Med Hyg* **78**, 837–838.
- 57 Ferrante A, Ljungstrom I and Lederer E (1988) Antitoxoplasmosis properties of sinefungin in mice. *C R Acad Sci* **306**, 109–113.
- 58 Majtan T, Pey AL and Kraus JP (2016) Kinetic stability of cystathionine beta-synthase can be modulated by structural analogs of S-adenosylmethionine: Potential approach to pharmacological chaperone therapy for homocystinuria. *Biochimie* **126**, 6–13.
- 59 Sasaki K *et al.* (2016) Inhibition of SET domain-containing lysine methyltransferase 7/9 ameliorates renal fibrosis. *J Am Soc Nephrol* **27**, 203–215.
- 60 Niitsuma M, Hashida J, Iwatsuki M, Mori M, Ishiyama A, Namatame M, Nishihara-Tsukashima A, Matsumoto A, Takahashi Y, Yamada H *et al.* (2010) Sinefungin VA and dehydrosinefungin V, new antitrypanosomal antibiotics produced by *Streptomyces* sp. K05-0178. *J Antibiot* **63**, 673–679.

- 61 Zhang J and Zheng YG (2016) SAM/SAH analogs as versatile tools for SAM-dependent methyltransferases. *ACS Chem Biol* **11**, 583–597.
- 62 Devkota K, Lohse B, Liu Q, Wang M-W, Stærk D, Berthelsen J and Clausen RP (2014) Analogues of the natural product sinefungin as inhibitors of EHMT1 and EHMT2. *ACS Med Chem Lett* **5**, 293–297.
- 63 Zheng W, Ibáñez G, Wu H, Blum G, Zeng H, Dong A, Li F, Hajian T, Allali-Hassani A, Amaya MF *et al.* (2012) Sinefungin derivatives as inhibitors and structure probes of protein lysine methyltransferase SETD2. *J Am Chem Soc* **134**, 18004–18014.
- 64 Liu Q, Cai X, Yang D, Chen Y, Wang Y, Shao L and Wang M-W (2017) Cycloalkane analogues of sinefungin as EHMT1/2 inhibitors. *Bioorg Med Chem* **25**, 4579–4594.
- 65 Hausmann S, Zheng S, Fabrega C, Schneller SW, Lima CD and Shuman S (2005) Encephalitozoon cuniculi mRNA cap (guanine N-7) methyltransferase: methyl acceptor specificity, inhibition BY S-adenosylmethionine analogs, and structure-guided mutational analysis. *J Biol Chem* **280**, 20404–20412.
- 66 Cai XC, Kapilashrami K and Luo M (2016) Synthesis and Assays of Inhibitors of Methyltransferases. *Methods Enzymol* **574**, 245–308. <https://doi.org/10.1016/bs.mie.2016.01.009>.
- 67 Tao Z (2018) Design, synthesis and in vitro anti-Zika virus evaluation of novel Sinefungin derivatives. *Eur J Med Chem* **157**, 994–1004.
- 68 Ferreira de Freitas R, Ivanochko D and Schapira M (2019) Methyltransferase inhibitors: competing with, or exploiting the bound cofactor. *Molecules* **24**, 4492.

## Supporting information

Additional supporting information may be found online in the Supporting Information section at the end of the article.

**Fig. S1.** hTR levels determined by RT-qPCR in the indicated human cell types. Bars represent fold change of hTR levels from three biological replicates, relative to the HeLa cell line and normalized to GAPDH. Error bars, SEM; the *P* values were determined by one-way ANOVA.

**Fig. S2.** (A) Population doubling of UMUC3 cells treated with the indicated concentrations of sinefungin from 2 biological replicates. Graph shows means with standard error. (B) hTERT levels determined by RT-qPCR in UMUC3 cells treated or not with 50  $\mu$ M sinefungin. Bars represent fold change of hTR levels from three biological replicates, relative to the untreated cell line and normalized to GAPDH. Error bars, SEM; No significant changes in hTERT abundance was observed in sinefungin treated cells; *P* value determined by Student's *T* test.

**Fig. S3.** (A, B) Population doubling of control and *PARN* KO cells treated with the indicated concentrations of sinefungin from 2 biological replicates. Graphs shows means with standard error. (C) RT-qPCR measurements of hTERT levels in control and *PARN* KO cell lines treated or not with 50  $\mu$ M sinefungin. Bars represent fold change of hTR levels from three biological replicates, normalized to untreated cells and relative to GAPDH. Error bar, SEM; the *P* values were nonsignificant and were determined by the Student's *t* test.